This article was downloaded by:
On: *25 January 2011*
Access details: *Access Details: Free Access*
Publisher *Taylor & Francis*
Informa Ltd Registered in England and Wales Registered Number: 1072954 Registered office: Mortimer House, 37-41 Mortimer Street, London W1T 3JH, UK

Separation Science and Technology
Publication details, including instructions for authors and subscription information:
http://www.informaworld.com/smpp/title~content=t713708471

Soil Cleanup by In-Situ Aeration. XXII. Impact of Natural Soil Organic Matter on Cleanup Rates

César Gómez-Lahoz[a]; José M. Rodriguez-Maroto[a]; David J. Wilson[b]
[a] DEPARTAMENTO DE INGENIERIA QUIMICA, FACULTAD DE CIENCIAS CAMPUS UNIVERSITARIO DE TEATINOS UNIVERSIDAD DE MALAGA, MALAGA, SPAIN [b] Department of Chemistry, Vanderbilt University, Nashville, USA

To cite this Article Gómez-Lahoz, César , Rodriguez-Maroto, José M. and Wilson, David J.(1995) 'Soil Cleanup by In-Situ Aeration. XXII. Impact of Natural Soil Organic Matter on Cleanup Rates', Separation Science and Technology, 30: 5, 659 — 682

To link to this Article: DOI: 10.1080/01496399508013885

URL: http://dx.doi.org/10.1080/01496399508013885

PLEASE SCROLL DOWN FOR ARTICLE

Full terms and conditions of use: http://www.informaworld.com/terms-and-conditions-of-access.pdf

This article may be used for research, teaching and private study purposes. Any substantial or systematic reproduction, re-distribution, re-selling, loan or sub-licensing, systematic supply or distribution in any form to anyone is expressly forbidden.

The publisher does not give any warranty express or implied or make any representation that the contents will be complete or accurate or up to date. The accuracy of any instructions, formulae and drug doses should be independently verified with primary sources. The publisher shall not be liable for any loss, actions, claims, proceedings, demand or costs or damages whatsoever or howsoever caused arising directly or indirectly in connection with or arising out of the use of this material.

SEPARATION SCIENCE AND TECHNOLOGY, **30**(5), pp. 659–682, 1995

Soil Cleanup by In-Situ Aeration. XXII. Impact of Natural Soil Organic Matter on Cleanup Rates

CÉSAR GÓMEZ-LAHOZ, JOSÉ M. RODRÍGUEZ-MAROTO,
and DAVID J. WILSON*
DEPARTAMENTO DE INGENIERIA QUIMICA
FACULTAD DE CIENCIAS
CAMPUS UNIVERSITARIO DE TEATINOS
UNIVERSIDAD DE MALAGA
29071 MALAGA, SPAIN

Downloaded At: 12:06 25 January 2011

ABSTRACT

A mathematical model for soil vapor extraction of volatile organic compounds from soils rich in natural humic organic carbon by means of a single vertical well screened along its length and operating underneath an impermeable cap is described. The model includes a distributed diffusion treatment of diffusion kinetics. Partitioning of volatile organic compounds between the aqueous phase and the natural organic carbon is handled by a linear isotherm or by a Freundlich isotherm. Freundlich isotherm exponents n_f chosen on the basis of published data lead to substantially more prolonged remediations than result from use of a similar linear isotherm.

INTRODUCTION

Soil vapor extraction (SVE) is now generally the technology of choice for the removal of volatile organic compounds (VOCs) from the vadose zone, and is also used with air sparging of the zone of saturation for capturing the VOCs released by sparging. EPA has published a number of reports which provide good introductions to the subject (Refs. 1 and 2, for example), and several comprehensive reviews have appeared (Ref.

---

* Permanent address: Department of Chemistry, Box 1822, Sta. B, Vanderbilt University, Nashville, TN 37235, USA.

Copyright © 1995 by Marcel Dekker, Inc.

Downloaded At: 12:06 25 January 2011

3, for example). The literature on SVE is now sufficiently extensive than a comprehensive review here would be inappropriate, and we have recently summarized the relevant literature on SVE modeling (4, 5).

The fraction of total natural organic carbon (f_c) present in the soil has been shown to play a very major role in the adsorption of VOCs by soils (Refs. 6 and 7, for instance), although Weber and his coworkers (8) have noted that some departure from a purely linear isotherm can be expected, and that experimental data are generally fitted better by a Freundlich isotherm than by a simple linear relationship. Meylan et al. (9) recently published a method for estimating soil sorption coefficients; their article also includes an extensive list of K_{oc} values. One expects that lack of information will continue to result in the use of the simple linear relationship because of insufficient data to support the fitting of a Freundlich isotherm, despite Weber's detailed and valid critique. Rutherford and Chiou (10), working with soil samples high in natural organics (muck and peat), found that the adsorption of carbon tetrachloride, trichloroethylene, and benzene from water and from the vapor phase followed linear isotherms, consistent with a partitioning of the solute VOC between two phases.

The importance of kinetic effects (both desorption and diffusion) should not be overlooked, as these can lead to SVE cleanup times which are far longer than those predicted by models which predict local equilibrium of VOC between the vapor phase and the stationary phases. Xing et al. (11) commented that slow sorption/desorption processes in soils are mainly the result of molecular diffusion into/from the more remote sorption sites in the organic matter in the three-dimensional structure. We have used models to explore the impacts of diffusion transport of VOC (Ref. 4, for example) and desorption kinetics (5) on SVE remediation rates, and a good deal of evidence is accumulating that these can be quite significant factors (12–17).

We here develop a model for the soil vapor extraction of VOCs from soils which are high in humic organic material. The model has radial one-dimensional geometry; a vertical pipe screened along its entire length extends from an overlying impermeable cap down nearly to the water table. The model includes the effects of diffusion kinetics in that we assume that we have low-permeability lenses of macroscopic thickness (0.5–5 cm or so), with the humic material being distributed more or less uniformly throughout the lens, as is the soil water. VOCs may be present in the lens in aqueous solution or "dissolved" in the humic organic phase. Within the volume subelements we assume local equilibrium between VOC in the humic phase and aqueous VOC, since mass transfer between these two phases involves 1) very low activation energies and 2) extremely short distances. Linear and Freundlich isothems are explored. The mathematical analysis is followed by simulation results illustrating the dependence of SVE cleanup times on the various parameters of the model. A short Conclusions Section completes the paper.

ANALYSIS

Development of the Modeling Equations

Let

C^c = total VOC concentration in condensed phases in the lenses, kg/m^3 of soil
C^w = aqueous VOC concentration in the lenses, kg/m^3 of water
C^a = VOC concentration in the organic carbon in the lenses, kg/m^3 of organic carbon
f_c = volume fraction organic carbon in the lenses, dimensionless
ω = water-filled porosity in the lenses, dimensionless
K_{oc} = VOC distribution coefficient between the organic carbon phase and the aqueous phase [dimensionless; (kg VOC/m^3 organic carbon phase)/(kg VOC/m^3 aqueous phase)]
K_{H} = Henry's constant of VOC in water, dimensionless
f_s = volume fraction of the total soil medium which is sand (i.e., highly permeable to air, containing little water and little humic material)
σ = porosity of sand
$2l$ = thickness of low-permeability structures containing water and humic material, m
ΔV_i = volume of ith volume element, m^3

Later we shall subscript concentrations appropriately to specify the volume element i and the slab k within the volume element as needed. See Fig. 1 for the geometry of the system; the model configuration is that of a single vertical well under an impermeable cap and screened along its entire length.

We assume local equilibrium between VOC in the aqueous and humic phases, so

$$C^a = K_{oc}C^w \tag{1}$$

In the lenses,

$$C^c = f_cC^a + \omega C^w \tag{2}$$

which, together with Eq. (1), gives

$$C^c = (f_cK_{oc} + \omega)C^w \tag{3}$$

Downloaded At: 12:06 25 January 2011

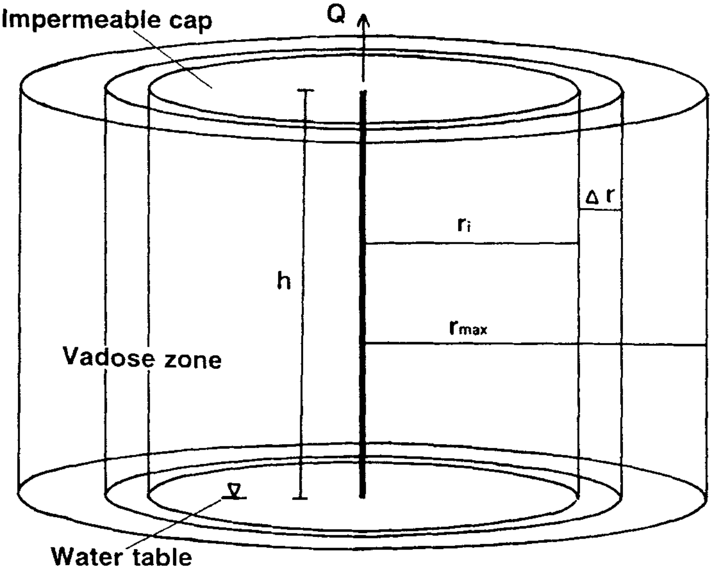

FIG. 1 Well geometry and notation.

Figure 2 shows a schematic diagram of a single volume element, with the mobile gas phase on the left and the stationary condensed phases partitioned into slabs in the usual way on the right. Let us examine diffusion in these slabs. A mass balance gives

$$\frac{(1-f_s)\Delta V_i}{n}\frac{dC^c_{ik}}{dt} = \frac{(1-f_s)\Delta V_i}{l} \times D\left[\frac{C^w_{i,k-1} - 2C^w_{ik} + C^w_{i,k+1}}{\Delta u}\right], \qquad k = 2, 3, \ldots, n-1 \tag{4}$$

which, on use of Eq. (3), yields

$$\frac{dC^c_{ik}}{dt} = \frac{1}{(f_c K_{oc} + \omega)}\frac{D}{(\Delta u)^2}(C^c_{i,k-1} - 2C^c_{ik} + C^c_{i,k+1}) \tag{5}$$

At the center of the lens we have

$$\frac{dC^c_{in}}{dt} = \frac{1}{(f_c K_{oc} + \omega)}\frac{D}{(\Delta u)^2}(C^c_{i,n-1} - C^c_{in}) \tag{6}$$

Downloaded At: 12:06 25 January 2011

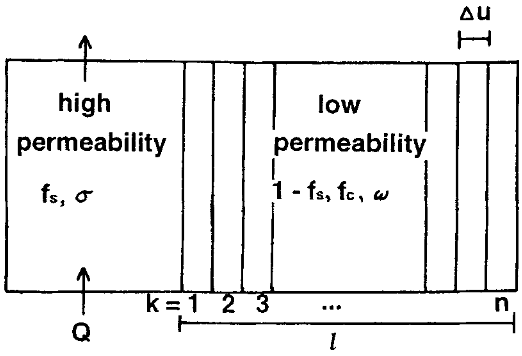

FIG. 2 A segment of a volume element showing mobile vapor phase and the slabs into which the low-permeability water-saturated porous structures are partitioned for analysis.

Downloaded At: 12:06 25 January 2011

For $k = 1$ (at the surface of the lens),

$$\frac{(1 - f_s)\Delta V_i}{n}\frac{dC_{i1}^c}{dt} = \frac{(1 - f_s)\Delta V_i}{l} D\left[\frac{C_{i2}^w - C_{i1}^w}{\Delta u} + \frac{C_i^g/K_\mathrm{H} - C_{i1}^w}{\Delta u/2}\right] \tag{7}$$

Use of Eq. (3) then gives

$$\frac{dC_{i1}^c}{dt} = \frac{D}{(f_cK_{oc} + \omega)(\Delta u)^2}(C_{i2}^c - C_{i1}^c) + \frac{2D}{(f_cK_{oc} + \omega)(\Delta u)^2}\left[\frac{(f_cK_{oc} + \omega)}{K_\mathrm{H}}C_i^g - C_{i1}^c\right] \tag{8}$$

Mass transport to the gas phase by diffusion from the condensed phases is given by

$$\sigma f_s \Delta V_i\left[\frac{\partial C_i^g}{\partial t}\right]_\mathrm{diff} = -\frac{(1 - f_s)\Delta V_i}{n}\frac{2D}{(f_cK_{oc} + \omega)(\Delta u)^2} \times \left[\frac{(f_cK_{oc} + \omega)}{K_\mathrm{H}}C_i^g - C_{i1}^c\right] \tag{9}$$

So

$$\left[\frac{\partial C_i^g}{\partial t}\right]_\mathrm{diff} = -\frac{(1 - f_s)}{\sigma f_s}\frac{2D}{(f_cK_{oc} + \omega)n(\Delta u)^2}\left[\frac{(f_cK_{oc} + \omega)}{K_\mathrm{H}}C_i^g - C_{i1}^c\right] \tag{10}$$

For the treatment of advection, we assume that the pressure drops are sufficiently small that the gas may be regarded as incompressible. Let

$$Q = \text{gas flow rate, m}^3\text{/s}$$

Then

$$\sigma f_s \Delta V_i \left[\frac{\partial C_i^g}{\partial t}\right]_{\text{adv}} = Q(C_{i+1}^g - C_i^g) \tag{11}$$

So finally

$$\frac{dC_i^g}{dt} = \frac{Q}{\sigma f_s \Delta V_i}(C_{i+1}^g - C_i^g) - \frac{(1 - f_s)}{\sigma f_s} \frac{2D}{(f_c K_{oc} + \omega) n (\Delta u)^2} \times \left[\frac{(f_c K_{oc} + \omega)}{K_{\text{H}}} C_i^g - C_{i1}^c\right] \tag{12}$$

This completes the construction of the modeling equations.

An Alternative Approach to the Handling of Diffusion in the Calculation

In connection with the modeling of diffusion transport, we were interested in testing a proposed Fourier series method which we hoped might in some circumstances permit faster calculation with no loss of accuracy. A discussion of this approach follows.

Our diffusion equation is Eq. (5), which in the limit as $n \to \infty$, $u \to 0$, becomes

$$\frac{\partial C_i^c(u, t)}{\partial t} = \frac{D}{(f_c K_{oc} + \omega)} \frac{\partial^2 C_i^c(u, t)}{\partial u^2} \tag{13}$$

The boundary conditions are

$$\frac{\partial C_i^c(l, t)}{\partial u} = 0 \tag{14}$$

and

$$C_i^c(0, t) = \frac{f_c K_{oc} + \omega}{K_{\text{H}}} C_i^g(t) \tag{15}$$

Define

$$D' = D/(f_c K_{oc} + \omega) \tag{16}$$

$$K'_{\text{H}} = K_{\text{H}}/(f_c K_{oc} + \omega) \tag{17}$$

Downloaded At: 12:06 25 January 2011

$$C = C_i^c \tag{18}$$

Our equations then become

$$\frac{\partial C}{\partial t} = D' \frac{\partial^2 C}{\partial u^2} \tag{19}$$

$$\frac{\partial C(l, t)}{\partial u} = 0 \tag{20}$$

$$C(0, t) = C_i^g(t)/K'_{\mathrm{H}} \tag{21}$$

Equation (19) is then solved by separation of variables in the usual way. Define

$$C(u, t) = C_0 + \sum C_\lambda(u, t) = C_0 + \sum U_\lambda(u)T_\lambda(t) \tag{22}$$

The boundary conditions require that

$$U_\lambda(0) = 0 \tag{23}$$

and

$$\frac{dU_\lambda(l)}{du} = 0 \tag{24}$$

If we set

$$C_0 = C_i^g(t)/K'_{\mathrm{H}} \tag{25}$$

and assume that $C_i^g(t)/K'_{\mathrm{H}}$ is a slowly varying function of t.

Since

$$C_\lambda(u, t) = U_\lambda(u)T_\lambda(t) \tag{26}$$

we have

$$\partial C/\partial t = U_\lambda \dot{T}_\lambda \tag{27}$$

and

$$\partial^2 C/\partial u^2 = U''_\lambda T_\lambda \tag{28}$$

Substituting and separating the variables then yields

$$\frac{\dot{T}_\lambda}{T_\lambda} = \frac{D' U''_\lambda}{U_\lambda} = -\lambda, \text{ a constant} \tag{29}$$

So

$$T_\lambda(t) = \exp(-\lambda t) \tag{30}$$

Downloaded At: 12:06 25 January 2011

Downloaded At: 12:06 25 January 2011

and

$$U''_\lambda + (\lambda/D')U_\lambda = 0 \tag{31}$$

So

$$U_\lambda(u) = A_\lambda \sin\sqrt{\lambda/D'}u + B_\lambda \cos\sqrt{\lambda/D'}u \tag{32}$$

From Eq. (23) we must have $B = 0$. From Eq. (24) we obtain

$$A_\lambda \sqrt{\lambda/D'} \cos\sqrt{\lambda/D'}l = 0 \tag{33}$$

from which we see that

$$\sqrt{\lambda/D'}l = (2n - 1)\pi/2, \qquad n = 1, 2, 3, \ldots \tag{34}$$

and

$$\lambda = \lambda_n = D'[(2n - 1)\pi/2l]^2 \tag{35}$$

Then

$$C(u, t) = C_0 + \sum_{n=1}^{\infty} A_n \sin\left[\frac{(2n-1)\pi u}{2l}\right]\exp\left\{-D'\left[\frac{(2n-1)\pi}{2l}\right]^2 t\right\} \tag{36}$$

Let us next determine the initial conditions to be used. We assume that we have equilibrium with respect to VOC mass transfer at time 0, and that we have no NAPL present. [Later it may be of interest to explore other initial conditions—NAPL present, and the condition in which we have NAPL and gaseous VOC in the sandy soil and no VOC in the lenses, which will allow us to explore the aging of a site before remediation.] For our case here,

$$C^{\text{tot}} = \sigma f_s C^g + \omega(1 - f_s)C^w + f_c(1 - f_s)C^a \tag{37}$$

$$C^g = K_H C^w \tag{38}$$

$$C^a = K_{oc} C^w \tag{39}$$

$$C^c = (f_c K_{oc} + \omega)C^w \tag{40}$$

So

$$C^{\text{tot}} = [\sigma f_s K_H + \omega(1 - f_s) + f_c(1 - f_s)K_{oc}]C^w \tag{41}$$

$$= \frac{[\sigma f_s K_H + \omega(1 - f_s) + f_c(1 - f_s)K_{oc}]}{(f_c K_{oc} + \omega)} C^c \tag{42}$$

and finally

$$C^c(u, 0) = \frac{(f_c K_{oc} + \omega)C^{\text{tot}}}{[\sigma f_s K_{\text{H}} + \omega(1 - f_s) + f_c(1 - f_s)K_{oc}]} \tag{43}$$

and also

$$C^g(0) = K_{\text{H}}C^w = \frac{K_{\text{H}}C^c}{f_c K_{oc} + \omega} = K'_{\text{H}}C^c \tag{44}$$

as expected.

We shall carry the integration out over time intervals τ, and shall develop a recursion formula for calculating the coefficients in the Fourier series. The procedure is as follows. One regards $C^g(t) = C_0 = C^g(p\tau)$ as constant in the interval $p\tau < t < (p + 1)\tau$, for which Eq. (36) has a set of coefficients A_n^p. Similarly, in the interval $(p + 1)\tau < (p + 2)\tau$, $C^g(t) = C^g[(p + 1)\tau]$, and Eq. (36) has another set of coefficients A_n^{p+1}. The solutions in the two intervals must be continuous in t at $t = (p + 1)\tau$, which will allow us to develop a recursion formula for the A_n^p. To start, in the time interval $0 < t < \tau$, we have

$$C(u, t) = C^g(0)/K'_{\text{H}} + 0 \tag{45}$$

from which we see that in the first time interval the A_n's, written as A_n^1 (for the first interval) are all zero. At $t = (p + 1)\tau$ we must match the solution in the interval $[p\tau, (p + 1)\tau]$ to the solution in the interval $[(p + 1)\tau, (p + 2)\tau]$. This gives

$$\frac{C^g[p\tau]}{K'_{\text{H}}} + \sum_{n=1}^{\infty} A_n^p \sin\left[\frac{(2n - 1)\pi u}{2l}\right]\exp\left\{-D'\left[\frac{(2n - 1)\pi}{2l}\right]^2 \tau\right\}$$
$$= \frac{C^g[(p + 1)\tau]}{K'_{\text{H}}} + \sum_{n=1}^{\infty} A_n^{p+1} \sin\left[\frac{(2n - 1)\pi u}{2l}\right] \tag{46}$$

This can be rearranged to give

$$\{C^g[p\tau] - C^g[(p + 1)\tau]\}/K'_{\text{H}}$$
$$= \sum_{n=1}^{\infty} \sin\left[\frac{(2n - 1)\pi u}{2l}\right]\left\{A_n^{p+1} - A_n^p \exp\left[-D'\left(\frac{(2n - 1)\pi}{2l}\right)^2 \tau\right]\right\} \tag{47}$$

Multiply Eq. (47) by sin $[(2m - 1)\pi u/2l]$, integrate from zero to 1, and solve for A_m^{p+1} to get

$$A_m^{p+1} = \frac{4}{(2m - 1)\pi}\{C^g[p\tau] - C^g[(p + 1)\tau]\}$$
$$/K'_{\text{H}} + A_m^p \exp\left[-D'\left(\frac{(2m - 1)}{2l}\right)^2 \tau\right] \tag{48}$$

Downloaded At: 12:06 25 January 2011

Downloaded At: 12:06 25 January 2011

Let us next determine the change of mass of VOC present in the aqueous and humic phases during the time interval between $p\tau$ and $(p + 1)\tau$.

$$m_i(t) = (1 - f_s)(\Delta V_i/l) \int_0^l C^c(u, t)du \tag{49}$$

$$m_i[(p + 1)\tau] - m_i[p\tau] = \Delta m_i$$

$$\Delta m_i = \frac{(1 - f_s)\Delta V_i}{l} \sum_{n=1}^{\infty} A_n^p \left\{ \exp\left[-D'\left(\frac{(2n - 1)}{2l}\right)^2 \tau \right] - 1 \right\} \times \int_0^l \sin\left[\frac{(2n - 1)\pi u}{2l}\right] du \tag{50}$$

which yields

$$\Delta m_i = (1 - f_s)\, \Delta V_i (2/\pi) \sum_{n=1}^{\infty} \frac{A_n^p}{(2n - 1)} \left\{ \exp\left[-D'\left(\frac{(2n - 1)\pi}{2l}\right)^2 \tau \right] - 1 \right\} \tag{51}$$

We note that

$$m_i(p\tau) = (1 - f_s)\Delta V_i (2/\pi) \sum_{n=1}^{\infty} \frac{A_n^p}{(2n - 1)} + \frac{C_i^g(p\tau)}{K_H'} \tag{52}$$

Next, let us examine the advective removal of VOC. For the *i*th volume element, during the time interval τ the net change on mass of VOC in the vapor phase is given by

$$\tau\sigma f_s \Delta V_i \left[\frac{dC_i^g}{dt}\right]_{\text{tot}} = Q(C_{i+1}^g - C_i^g)\tau - \Delta m_i \tag{53}$$

so

$$\frac{dC_i^g}{dt} = \frac{Q}{\sigma f_s \Delta V_i} (C_{i+1}^g - C_i^g) - \frac{\Delta m_i}{\tau\sigma f_s \Delta V_i} \tag{54}$$

If we wish to use the steady-state approximation for C_i^g, we set the left-hand side of Eq. (53) equal to zero and solve for C_i^g; this yields

$$C_i^g = C_{i+1}^g - (\Delta m_i/Q\tau) \tag{55}$$

The modeling then involves calculation of the Δm_i from Eq. (51), of the m_i from Eq. (52), of the C_i^g from Eq. (54) or (55), and, lastly, of the A_n^{p+1} from Eq. (48). This completes the iterative loop.

The total residual mass of VOC at any time is given by

$$M_{\text{tot}} = \sum_{i=1} m_i + \sigma f_s \Delta V_i C_i^g \tag{56}$$

and the VOC concentration in the effluent soil gas is given by

$$C_{\text{effl}} = C_1^g \tag{57}$$

This completes the model.

Modeling with the Freundlich Isotherm

The data presented by Weber and his coworkers (8) provides convincing evidence that the Freundlich isotherm often provides a significantly better fit to adsorption data for high-organics soils than does the linear isotherm. One notes with some regret that the extra time and expense involved in obtaining the data necessary to estimate the two parameters required by the Freundlich isotherm will probably continue to preclude its use in most applications. It is of interest to have some idea of the extent to which use of the linear isotherm instead of the Freundlich affects the results of modeling calculations. The mean value and standard deviation of the Freundlich exponent calculated from the values given in Ref. 8 are 0.838 and 0.124, respectively.

In this section we extend the model described above to permit its use with the Freundlich isotherm. Notation is as used previously, with a few additions. We write the Freundlich isotherm as

$$C^a = K_f (C^w)^{nf} \tag{58}$$

where K_f = Freundlich isotherm coefficient, $(\text{kg/m}^3)^{1-nf}$
n_f = Freundlich isotherm exponent, dimensionless

The total VOC concentration is given by

$$C_{\text{tot}} = \sigma f_s C^g + (1 - f_s)[\omega C^w + f_c C^a] \tag{59}$$

which, on use of Henry's law and the Freundlich isotherm, yields

$$C_{\text{tot}} = \sigma f_s K_H C^w + (1 - f_s)\omega C^w + (1 - f_s) f_c K_f (C^w)^{nf} \tag{60}$$

This can be solved iteratively for C_w by the scheme

$$C^w = \left[\frac{C_{\text{tot}} - [\sigma f_s K_H + (1 - f_s)\omega]C^w}{(1 - f_s) f_c K_f}\right]^{1/nf} \tag{61}$$

Initially, C_w is set equal to zero on the left-hand side to start the iteration.

Downloaded At: 12:06 25 January 2011

Downloaded At: 12:06 25 January 2011

The total VOC concentration in condensed phases in the *j*th slab of the *i*th volume element is given by

$$C_{ij}^{c} = \omega C_{ij}^{w} + f_c C_{ij}^{a} \tag{62}$$

This, on use of the Freundlich isotherm, gives

$$C_{ij}^{c} = \omega C_{ij}^{w} + f_c K_f (C_{ij}^{w})^{nf} \tag{63}$$

from which C_{ij}^{w} is calculated iteratively by use of

$$C_{ij}^{w} = \left[\frac{C_{ij}^{c} - \omega C_{ij}^{w}}{f_c K_f}\right]^{1/nf} \tag{64}$$

The equations describing diffusion transport of VOC within the lenses are

$$\frac{dC_{ij}^{c}}{dt} = \frac{D}{\Delta u^2}[C_{i,j+1}^{w} - 2C_{i,j}^{w} + C_{i,j-1}^{w}], \qquad j = 2, 3, \ldots, n - 1 \tag{65}$$

$$\frac{dC_{in}^{c}}{dt} = \frac{D}{\Delta u^2}[-C_{i,n}^{w} + C_{i,n-1}^{w}] \tag{66}$$

$$\frac{dC_{i1}^{c}}{dt} = \frac{D}{\Delta u^2}[C_{i,2}^{w} - C_{i,1}^{w} + 2(C_i^{g}/K_{\mathrm{H}} - C_{i1}^{w})] \tag{67}$$

A mass balance for vapor phase VOC in the *i*th volume element gives

$$\sigma f_s \Delta V_i \frac{dC_i^{g}}{dt} = Q(C_{i+1}^{g} - C_i^{g}) + \frac{(1 - f_s)\Delta V_i}{l} D\left[\frac{2(C_{i1}^{w} - C_i^{g}/K_{\mathrm{H}})}{\Delta u}\right] \tag{68}$$

As before, we make the steady-state assumption for C_i^{g}, setting the left-hand side of Eq. (68) equal to zero and solving for C_i^{g}; the result is

$$C_i^{g} = \left[C_{i+1}^{g} + \frac{2(1 - f_s)\Delta V_i D}{l\Delta u Q} C_{i1}^{w}\right] \Bigg/ \left[1 + \frac{2(1 - f_s)\Delta V_i D}{l\Delta u Q K_{\mathrm{H}}}\right] \tag{69}$$

The remainder of the analysis is carried out exactly as before.

RESULTS

The model was implemented in TurboBASIC and run on an AlphaSystem microcomputer using an 80486 microprocessor running at 50 MHz. Four versions of the model were investigated: 1) the differential equations were used without modification; 2) the steady-state approximation was used for the advective equations (for the C_i^gs) and the differential equations were used to handle diffusion in the lenses; 3) the differential equations were used for the C_i^gs and the Fourier series approach was used to handle diffusion in the lenses; and 4) the steady-state approximation was used for the C_i^gs and the Fourier series approach was used for diffusion in the lenses. It was desired to determine which of these algorithms is the fastest, given that accurate results for both total residual VOC mass and the effluent soil gas VOC concentration must be obtained. The parameter set used in these runs is given in Table 1.

The four algorithms were run with ranges of the time increment Δt, with the results shown in Table 2. The results indicate that much is to be gained in computing speed by using the steady-state approximation. This permits one to avoid the constraint $\Delta t < \Delta r/v$ (where Δr is the distance increment and v is the linear gas velocity of the system) which severely limits the time increments which can be used when the C_i^gs are calculated from the differential equations. The maximum value of Δt which could be used for both Algorithm 1 and Algorithm 3 with these parameters was

Downloaded At: 12:06 25 January 2011

TABLE 1
Default Parameters Used in the Algorithm Test Runs and in the Runs Using Linear and Freundlich Isotherms for VOC on Soil Organic Carbon

Domain radius	10 m
Depth of well	8 m
Gas flow rate	50 SCFM
Gas flow rate	0.02336 m^3/s
Porosity of air-filled soil, σ	0.3
Volume fraction of soil which is air-filled, f_s	0.4
Volume fraction of organic carbon in the lenses, f_c	0.05
Water-filled porosity in lenses, ω	0.3
Soil density	1.7 g/cm^3
Thickness of lenses	4 cm
VOC	Trichloroethylene
VOC density	1.46 g/cm^3
VOC diffusivity in the wet lenses	2.0×10^{-10} m^2/s
VOC Henry's constant (dimensionless)	0.2821
Organic carbon/water partition coefficient of VOC	25
Initial VOC concentration	100 mg/kg of soil
n_r	10
Number of slabs in diffusion modeling	6
Number of terms in Fourier series	10
Initial effluent soil gas VOC concentration	0.1619 kg/m^3
Initial total mass of VOC	427.26 kg

TABLE 2
Effects of the Magnitude of Δt on Algorithm Performance

Algorithm	Δt (seconds)	Remarks
1	2,700	Unstable for both M_{tot} and C_{effl}
	675	M_{tot} OK, C_{effl} unstable
	275	M_{tot} OK, C_{effl} unstable
	250	M_{tot} OK, C_{effl} OK
2	27,000	M_{tot} OK, C_{effl} unstable at start of run
	13,500	M_{tot} OK, C_{effl} OK
	20,000	M_{tot} OK, C_{effl} OK
3	300	M_{tot} OK, C_{effl} unstable
	275	M_{tot} OK, C_{effl} unstable
	250	M_{tot} OK, C_{effl} OK
4	13,500	M_{tot} OK, C_{effl} irregular at start of run
	6,750	M_{tot} OK, C_{effl} irregular at start of run
	3,375	M_{tot} OK, C_{effl} irregular at start of run
	1,000	M_{tot} OK, C_{effl} slightly irregular at start of run

Downloaded At: 12:06 25 January 2011

250 seconds, while the maximum value of Δt which could be used with algorithm 2 was 20,000 seconds.

Somewhat to our surprise, use of the Fourier series approach to diffusion with the steady-state approximation for the C_i^gs (Algorithm 4) yielded results which were less satisfactory than those obtained by the simpler Algorithm 2, at least with the parameter set used. Algorithm 4 was quite satisfactory for calculating the total residual contaminant mass; however, it showed worrisome irregularities in the effluent soil gas VOC concentrations for the first few hours of the simulation. It was hoped that Algorithm 4 would show better performance in terms of computing speed by permitting the use of larger values of Δt than can be used with Algorithm 2, but in the runs reported here this was not the case. We conclude that Algorithm 2, based on the steady-state approximation for the calculation of the C_i^gs and the differential equations for the modeling of diffusion transport, is the most satisfactory of the four algorithms tested in terms of computation time requirements, and that all the algorithms yield virtually identical results for sufficiently small values of the time increments. The simulations discussed below were all run with Algorithm 2. The default values of the parameters are given in Table 1, and a value of Δt of 6750 seconds was used in all runs.

In Fig. 3 we see the effect of f_c, the fraction of the soil in the wet lenticular structures which is natural organic carbon. The values of f_c are

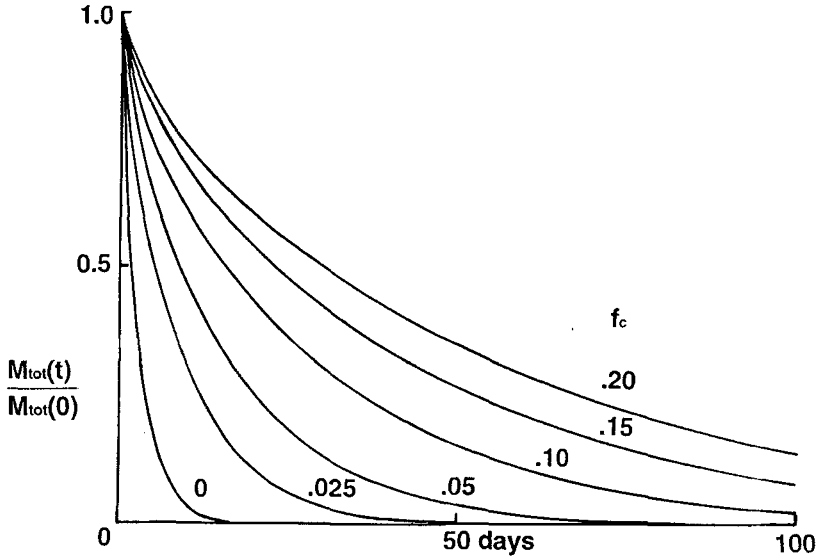

FIG. 3 Plots of $M_{tot}(t)/M_{tot}(0)$ versus t; effect of volume fraction of natural organic carbon, f_c. f_c = 0, .025, .05, .10, .15, and .20, from the bottom up. Other parameters as in Table 1.

Downloaded At: 12:06 25 January 2011

0, 0.05, 0.10, 0.15, and 0.20. As expected, plots of $M_{tot}(t)/M_{tot}(0)$ show spectacular increases in cleanup time with increasing f_c. Figure 4 shows plots of $C_{effl}(t)/C_{effl}(0)$ and $M_{tot}(t)/M_{tot}(0)$ for f_c = 0.15; the effluent soil gas concentration initially falls off rapidly, and then exhibits very marked tailing.

The effect of the organic carbon/water partition coefficient K_{oc} is shown in Fig. 5; runs having K_{oc} = 10, 25, 50, 75, and 100 are shown. We see the expected decrease in the rate of cleanup as the ability of the natural organic carbon to bind VOCs is increased. The results shown in Figs. 3 and 5 indicate that, if any appreciable amount of natural organic carbon is present in the soil, this will be one of the dominant factors controlling the desorption of VOCs.

The thickness l of the wet, organic carbon-containing lenticular structures also has a profound effect on the rate of VOC desorption, as seen in Fig. 6. In the runs shown here, l = 2, 3, 4, 5, and 6 cm. As expected, cleanup times are roughly proportional to the square of the lens thickness.

Since these systems are definitely in the diffusion-limited regime, we do not expect changes in the gas flow rate Q to have much of an effect

Downloaded At: 12:06 25 January 2011

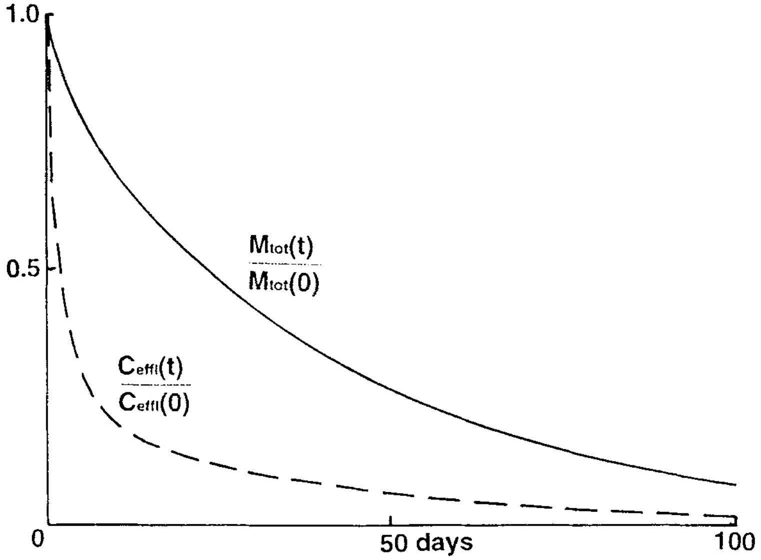

FIG. 4 Plots of $M_{tot}(t)/M_{tot}(0)$ and $C_{effl}(t)/C_{effl}(0)$ versus t. f_c = .15. Other parameters as in Table 1.

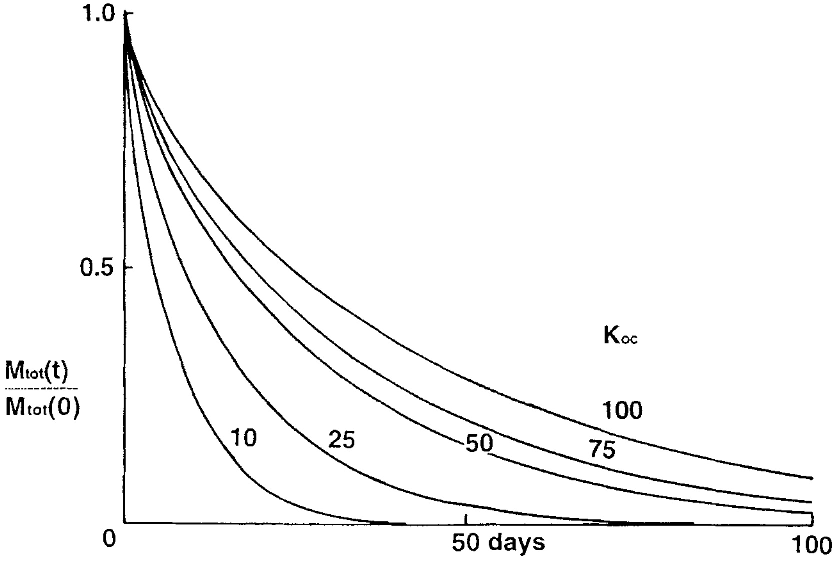

FIG. 5 Plots of $M_{tot}(t)/M_{tot}(0)$ versus t; effect of the organic carbon/water partition coefficient K_{oc}. K_{oc} = 100, 75, 50, 25, and 10, from the top down. Other parameters as in Table 1.

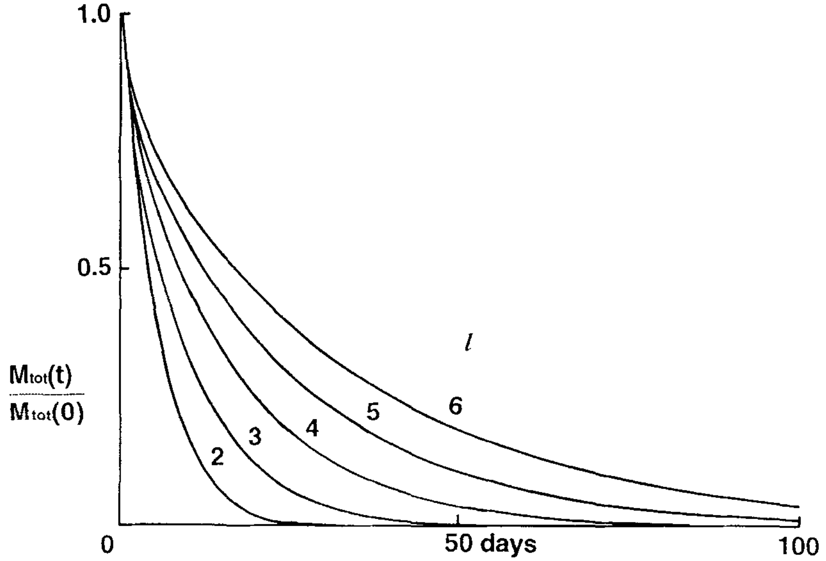

FIG. 6 Plots of $M_{tot}(t)/M_{tot}(0)$ versus t; effect of thickness of low-permeability water-saturated lenses. $2l$ = 6, 5, 4, 3, and 2 cm, from the top down. Other parameters as in Table 1.

Downloaded At: 12:06 25 January 2011

on cleanup time until substantial reductions have been made. In agreement with this assessment, the runs shown in Fig. 7 show relatively little effect of gas flow rate on cleanup time until Q is decreased from 12.5 to 6.25 SCFM

Figure 8 shows the effect of the value of the Henry's constant K_H on VOC removal rate. The Henry's constants range from 0.015625 to 1.0 by factors of 2 in these runs. Here Q = 50 SCFM, so the system is approaching the diffusion-limited regime. We therefore see relatively little effect on cleanup rate of K_H until it is reduced down to 0.03125, at which point the cleanup rate starts to decrease significantly. The independence of cleanup rate from the Henry's constant under diffusion-limited conditions was noted earlier by Sellers and Schreiber (18) in connection with the air sparging of VOCs.

On the other hand, the rate of remediation is quite strongly dependent on K_H if the air flow rate is decreased to 6.25 SCFM, as seen in Fig. 9. As in Fig. 8, the Henry's constants range from 0.015625 to 1.0 by factors of 2 in these runs. For a simple one-compartment equilibrium-controlled

Downloaded At: 12:06 25 January 2011

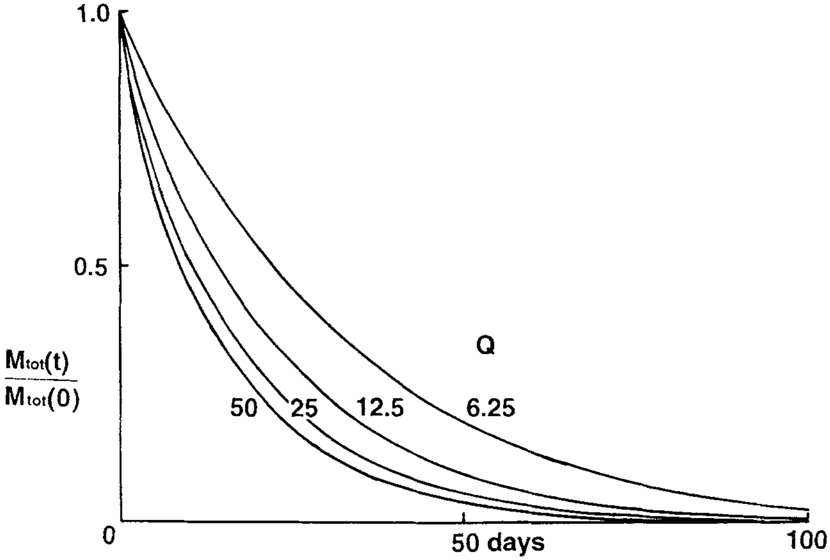

FIG. 7 Plots of $M_{tot}(t)/M_{tot}(0)$ versus t; effect of air flow rate. Q = 6.25, 12.5, 25, and 50 SCFM, from the top down. Other parameters as in Table 1.

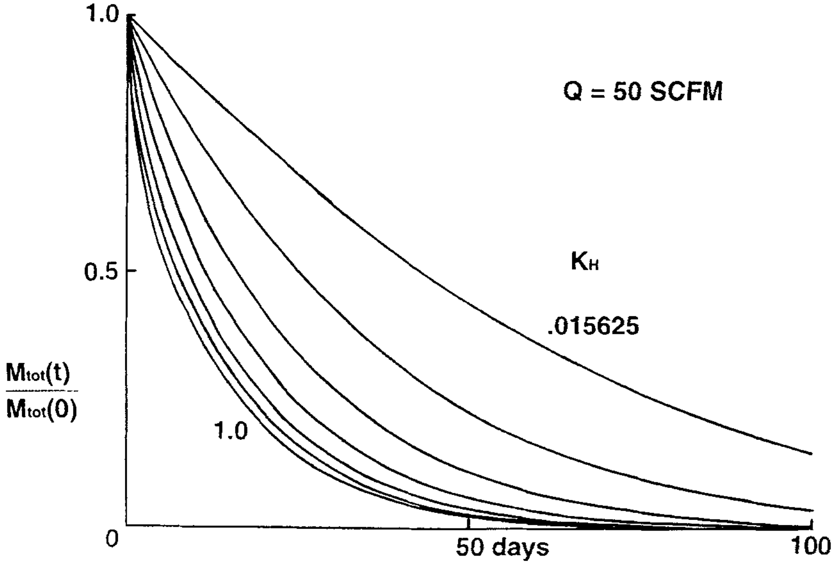

FIG. 8 Plots of $M_{tot}(t)/M_{tot}(0)$ versus t; effect of Henry's constant at a gas flow rate Q of 50 SCFM. K_H = 1, .5, .25, .125, .0625, .03125, and .015625, from the bottom up. Other parameters as in Table 1.

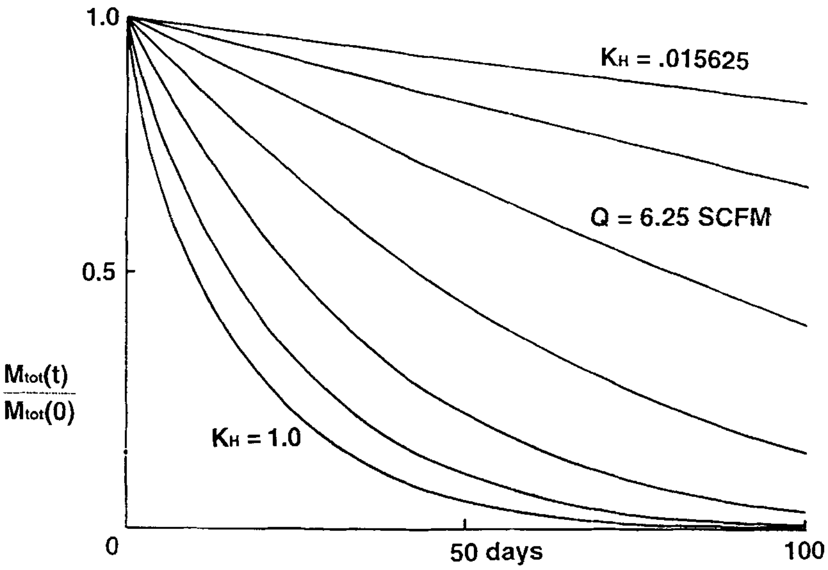

FIG. 9 Plots of $M_{\mathrm{tot}}(t)/M_{\mathrm{tot}}(0)$ versus t; effect of Henry's constant at a gas flow rate Q of 6.25 SCFM. K_{H} = 1, .5, .25, .125, .0625, .03125, and .015625, from the bottom up. Other parameters as in Table 1.

Downloaded At: 12:06 25 January 2011

model, $M_{\mathrm{tot}}(t)$ is given by

$$M_{\mathrm{tot}}(t) = M_{\mathrm{tot}}(0) \exp\left[- \frac{QK_{\mathrm{H}}}{V(f_c K_{oc} + \omega + \sigma K_{\mathrm{H}})} t \right] \tag{70}$$

so the strong dependence of cleanup rate on K_{H} at low flow rates is certainly not surprising. Here V is the volume of soil being aerated and the other symbols are as previously defined. It is assumed here that the soil is homogeneous.

Figures 10–12 show runs exploring the effects of using the Freundlich isotherm. Default values of the parameters are given in Table 1. The effect of K_f at constant n_f is shown in Fig. 10; in these runs K_f = 12.5, 25, and 50 $(\mathrm{kg/m^3})^{1-nf}$ and n_f = 0.838, the mean of the 18 values reported in Ref. 8. The larger the value of K_f, the larger the capacity of the natural organic carbon to retain VOCs, so we expect the decrease in cleanup rate observed with increasing K_f.

The effect of n_f at constant K_f is shown in Fig. 11. In these runs the numerical value of K_f is held constant at 25, and n_f = 0.714, 0.838, 0.962, and 1.0 (a linear isotherm). At low VOC concentrations the Freundlich

Downloaded At: 12:06 25 January 2011

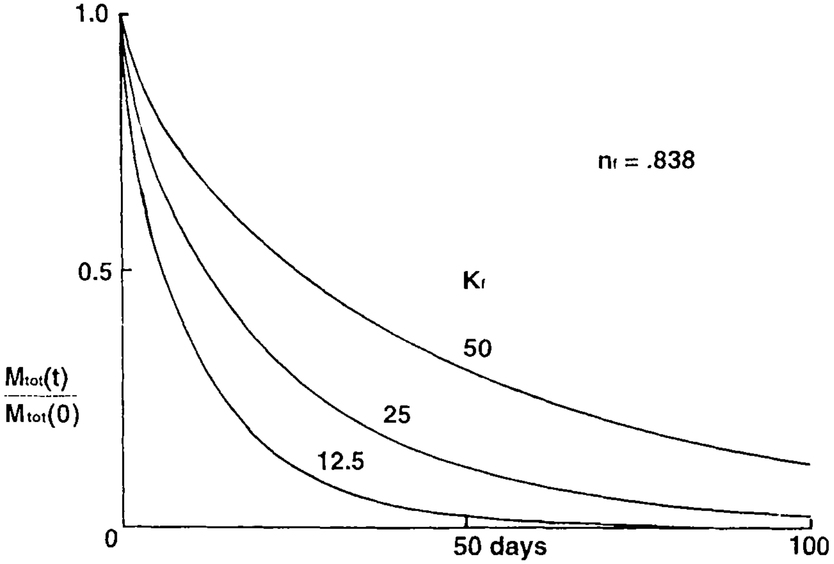

FIG. 10 Plots of $M_{tot}(t)/M_{tot}(0)$ versus t for Freundlich isotherm runs; effect of K_f. K_f = 50, 25, and 12.5, from the top down; n_f = .838. Other parameters as in Table 1.

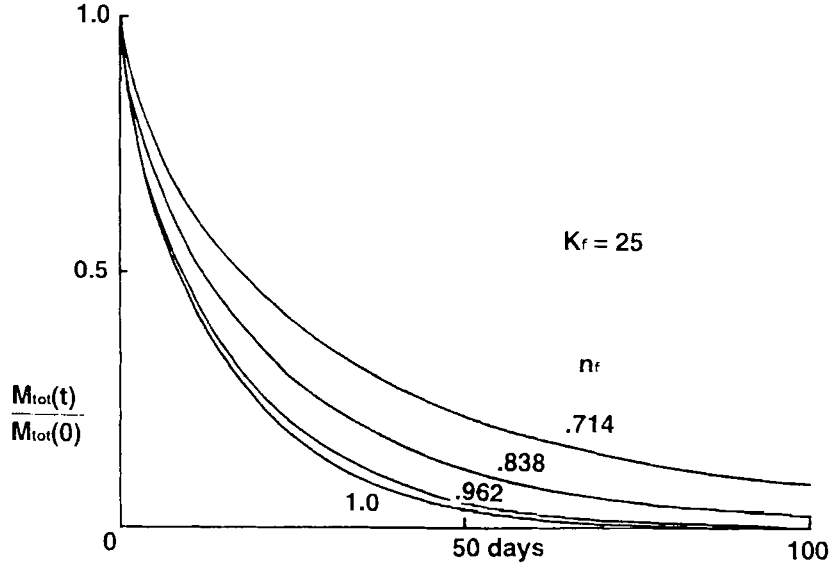

FIG. 11 Plots of $M_{tot}(t)/M_{tot}(0)$ versus t for Freundlich isotherm runs; effect of n_f. n_f = .714, .838, .962, and 1.0, from the top down; K_f = 25 $(\mathrm{kg/m^3})^{1-n_f}$. Other parameters as in Table 1.

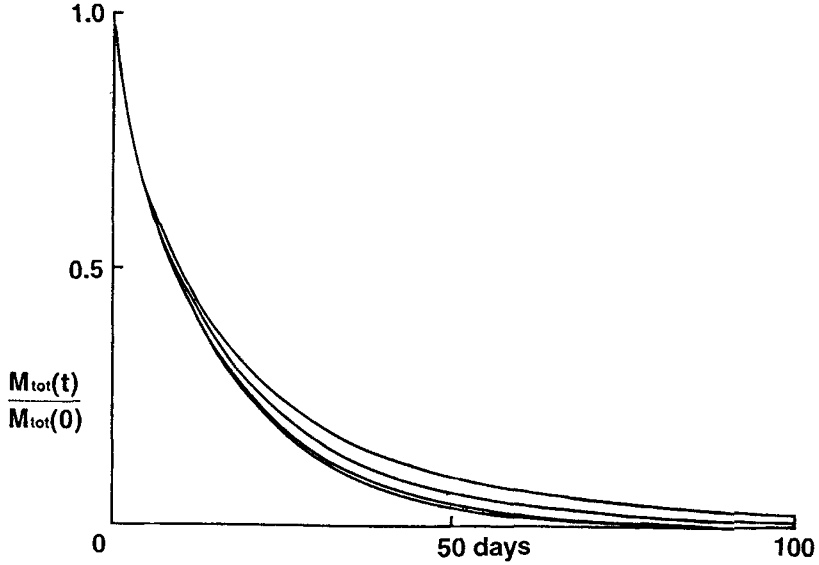

FIG. 12 Plots of $M_{\text{tot}}(t)/M_{\text{tot}}(0)$ versus t for Freundlich isotherm runs; effect of joint variation of n_f and K_f. (n_f, K_f) = (.714, 15.2159), (.838, 18.9160), (.962, 23.4633), and (1.0, 25), from the top down. Other parameters as in Table 1. These values are chosen to give an initial gas phase VOC concentration of 0.0498 kg/m^3.

Downloaded At: 12:06 25 January 2011

isotherm binds more VOC the smaller the value of n_f, so the observed drastic increase in tailing as n_f decreases from 1.0 to 0.714 is what is expected. The values of 0.714 and 0.962 are one standard deviation unit below and above the mean value of n_f, 0.838. It is difficult to give a more detailed interpretation of these runs since, while the numerical value of K_f is being held constant, its units depend on the value of n_f selected.

In Fig. 12 values of n_f of 1.0, 0.962, 0.838, and 0.714 were used and values of K_f were selected to give an initial equilibrium gas phase concen-

TABLE 3
Values of n_f and K_f Used in Fig. 12 and Giving an Initial Equilibrium Gas Phase VOC Concentration of 0.0498 kg/m^3

n_f	K_f
1.000	25.0
0.962	23.4633
0.838	18.9160
0.714	15.2159

tration in all runs of 0.0498 kg/m^3; the values of K_f are given in Table 3. The remediation rates are observed to decrease with decreasing values of n_f, as was observed in Fig. 11, but the effect is not as large. It is evident, however, that n_f values realistically selected in the light of the data of Weber and his coworkers result in considerably more tailing of the cleanup than is found when a linear isotherm is used. This additional tailing is the result of the equilibrium isotherm used; the tailing observed in the run for which $n_f = 1$ is mainly associated with the kinetics of VOC diffusion transport.

CONCLUSIONS

The results obtained with this model for the SVE of soils containing natural humic organic matter lead to the following conclusions.

- Models in which the steady-state approximation is used for the calculation of gas phase VOC concentrations compute roughly 100 times more rapidly than models in which the differential equations are used to calculate the gas phase concentrations. There is negligible loss of accuracy in using the steady-state approximation.
- Use of a Fourier series approach to handle diffusion transport does not appear to be advantageous.
- The model results indicate that one may expect large decreases in cleanup rates with increasing natural organic carbon content of the soil.
- Cleanup rates show large decreases with increasing thickness of low-permeability porous structures from which VOC must be transported by diffusion through an aqueous phase; this feature is common to all of our SVE models which include distributed diffusion.
- As seen in our earlier models, increasing the gas flow rate in an SVE well has little effect if diffusion transport is the rate-limiting step in the removal of VOC.
- Cleanup rate is essentially proportional to the Henry's constant K_H if the gas flow rate is sufficiently slow that the SVE is equilibrium-controlled. Cleanup rate approaches independence of K_H as the gas flow rate increases to the point where the SVE is diffusion-controlled.
- Realistic values of the Freundlich exponent n_f increase tailing markedly over what is found with linear isotherms. This component of the tailing is not associated with diffusion transport, but with the adsorption isotherm itself. Assessment of such tailing requires either that Freundlich isotherm parameters be determined for the soil to be treated by SVE, or that pilot SVE runs be carried out nearly to completion.

Downloaded At: 12:06 25 January 2011

Use of a linear isotherm may result in serious underestimation of the cleanup time.

ACKNOWLEDGMENTS

D.J.W. is greatly indebted to the University of Malaga for its hospitality and the use of its facilities, to Dr. J. J. Rodríguez-Jimenez for making his visit to Malaga possible and for helpful discussions of the project, to Vanderbilt University for financial support during his leave, and to the Spanish Government (DGICYT) for a fellowship in support of this work.

REFERENCES

1. T. A. Pedersen and J. T. Curtis, *Soil Vapor Extraction Technology Reference Handbook*, Risk Reduction Engineering Laboratory, US EPA Report EPA/540/2-91/003, 1991.
2. J. P. Stumbar and J. Rawe, *Guide for Conducting Treatability Studies under CERCLA: Soil Vapor Extraction Interim Guidance*, US EPA Report EPA/540/2-91/019A, 1991.
3. D. J. Wilson and A. N. Clarke, "Soil Vapor Extraction," in *Hazardous Waste Site Soil Remediation: Theory and Application of Innovative Technologies* (D. J. Wilson and A. N. Clarke, Eds.), Dekker, New York, 1993, p. 171.
4. D. J. Wilson, J. M. Rodríguez-Maroto, and C. Gómez-Lahoz, "Soil Cleanup by In-Situ Aeration. XIX. Effects of Spill Age on Soil Vapor Extraction Remediation Rates," *Sep. Sci. Technol.*, *29*, 1645 (1994).
5. J. M. Ródriguez-Maroto, D. J. Wilson, and C. Gómez-Lahoz, "Soil Cleanup by In-Situ Aeration. XXI. Effects of Desorption Rates and Equilibria on Remediation Rates," *Ibid.*, *30*, 521 (1995).
6. L. J. Thibodeaux, *Chemodynamics: Environmental Movement of Chemicals in Air, Water and Soil*, Wiley-Interscience, New York, 1979.
7. W. J. Lyman, W. F. Reehl, and D. H. Rosenblatt (Eds.), *Handbook of Chemical Property Estimation Methods*, American Chemical Society, Washington, D.C., 1990, Chap. 4.
8. W. J. Weber Jr., P. M. McGinley, and L. E. Katz, "A Distributed Reactivity Model for Sorption by Soils and Sediments. 1. Conceptual Basis and Equilibrium Assessments," *Environ. Sci. Technol.*, *26*, 1955 (1992).
9. W. Meylan, P. H. Howard, and R. S. Boethling, "Molecular Topology/Fragment Contribution Method for Predicting Soil Sorption Coefficients," *Ibid.*, *26*, 1560 (1992).
10. D. W. Rutherford and G. T. Chiou, "Effect of Water Saturation in Soil Organic Matter on the Partition of Organic Compounds," *Ibid.*, *26*, 965 (1992).
11. B. Xing, W. B. McGill, M. J. Dudas, Y. Maham, and L. Hepler, "Sorption of Phenol by Selected Biopolymers: Isotherms, Energetics, and Polarity," *Ibid.*, *28*, 466 (1994).
12. S. G. Pavlostathis and G. N. Mathavan, "Desorption Kinetics of Selected Volatile Organic Compounds from Field Contaminated Soils," *Ibid.*, *26*, 532 (1992).
13. C. J. Werth, J. Farrell, and M. Reinhard, "The Effects of Temperature on the Slow Desorption of Trichloroethylene from Livermore Sand, Clay and Bulk Fractions: Isotherms and Kinetics," in *Preprint Extended Abstract, Division of Environmental Chemistry, American Chemical Society, San Diego, CA, March 13–18, 1994*, p. 350.

Downloaded At: 12:06 25 January 2011

14. T. C. Harmon and B. K. Dela Barre, "The Effect of Temperature on the Rate of Desorption of Halogenated Alkenes from Aquifer Solids," *Ibid.*, p. 343.
15. B. K. N. Njoroge, R. S. Cherry, and W. P. Ball, "Effects of Soil Development and Morphology on the Sorption of Nonpolar Organic Compounds," *Ibid.*, p. 331.
16. B. A. Holmen and P. M. Gschwend, "Evaluation of Sorption Kinetics in an Atlantic Coastal Plain Aquifer Sand," *Ibid.*, p. 339.
17. T. M. Young, M. A. Schlautman, and W. J. Weber Jr., "Effect of Soil Characteristics on Sorption Energetics of Hydrophobic Organic Compounds," *Ibid.*, p. 335.
18. K. L. Sellers and R. P. Schreiber, "Air Sparging Model for Predicting Groundwater Cleanup Rate," in *Proceedings, Conference on Petroleum Hydrocarbons and Organic Chemicals in Ground Water: Prevention, Protection and Restoration. Eastern Regional Ground Water Issues, Houston, TX, November 4–6, 1992.*

Received by editor July 27, 1994

Downloaded At: 12:06 25 January 2011